I

RAPPORTS INTRODUCTIFS / EINFÜHRUNGSBERICHTE / INTRODUCTORY REPORTS

The Ultimate Load Behaviour of Plate Girders Loaded in Shear

Comportement à la ruine des poutres à âme pleine soumises au cisaillement

Traglastverhalten schubbeanspruchter Blechträger

K.C. ROCKEY
M.Sc., Ph.D., C.Eng., F.I.C.E.
Professor of Civil and Structural Engineering
University College, Cardiff, England

M. ŠKALOUD
Doc., C.Sc., Ing.
Senior Research Fellow
Czechoslovak Academy of Sciences
Institute of Theoretical and Applied Mechanics
Prague, Czechoslovakia

1. INTRODUCTION

The paper presents a Plastic Method of Design for Plate Girder Webs which allows for the influence of flange rigidity upon the post buckled behaviour of webs. The design procedure which is based on a study of the behaviour of 40 plate girders tested by the authors, has been checked against other experimental data available in the Technical Press. Because the present design procedure allows for the influence of flange stiffness upon the post buckled behaviour of shear webs it is more accurate than existing design methods.

Although plastic design methods have been developed for linear and flat slab structures, the majority of specifications used for the design of plate girders are still based on the concept of a limiting elastic stress. Since such design methods cannot result in optimum structures there has been an urgent need for a plastic collapse method for plate girders whose webs buckle prior to failure. The present paper presents a method for calculating the ultimate load of plate girders loaded in shear which allows for the influence which the stiffness of the flange members has upon the post buckled behaviour of the webplates.

Previous studies (1-5) involving the elastic post buckled behaviour of webplates loaded in shear have shown that the post-buckled behaviour of a shear panel is greatly influenced by the influence of the flexural rigidity of the flanges and the stiffness of the vertical stiffeners.

The theoretical study of Leggett and Hopkins on the behaviour of infinitely long plates showed how the stress distribution and the inclination of the waves developed in the buckled web varied significantly with both the flexural stiffness of the flanges and the cross sectional area of the vertical stiffeners.

In 1957, Rockey[3] reported on an extensive study of the elastic post buckled behaviour of shear webs having aspect ratios (b/d) of 2 and 3. This study established that if the flange flexural stiffness was such that the flange stiffness parameter $I/_b 3_t$ was less than the value given by equation (1) then due to the inward deflection of the flanges the depth of the buckles increased considerably.

$$I/_b 3_t = A\left(\frac{\tau}{\tau_{cr}} - 1\right) \quad \ldots\ldots\ldots\ldots\ldots (1)$$

where A = 0.00035.

As a result of subsequent studies by Djubek[4], Rockey and Martin[5], it was noted that the minimum value of A in equation 1 varied with the aspect ratio b/d in the manner shown in Figure 1.

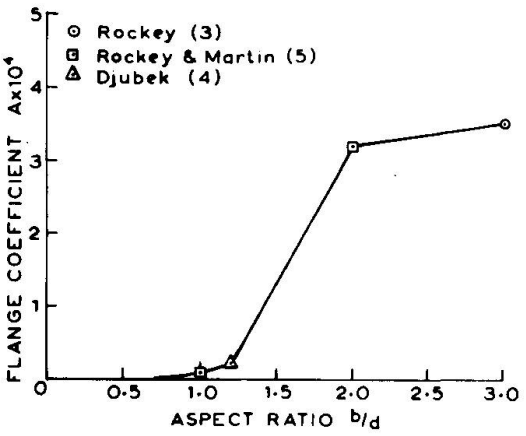

FIG. 1. VARIATION OF THE COEFFICIENT A IN EQUATION (1) WITH THE ASPECT RATIO b/d

In 1960, Basler and his colleagues (6-9) at Lehigh presented an ultimate method of design for shear webs for the particular case where the flanges are considered to be very flexible. They assumed that due to the flexibility of the flanges the buckles slip into the off diagonal form shown in Figure 2(a) and that failure occurs when the shaded area yields.

Using this structural model, Basler obtained the following expression for the ultimate load of a shear panel :-

$$W_{ult} = dt\left[\tau_{cr} + \frac{\sqrt{3}\,\tau_{yw}}{2\sqrt{1+\alpha^2}}\left(1 - \frac{\tau_{cr}}{\tau_{yw}}\right)\right] \quad \ldots\ldots\ldots\ldots\ldots (2)$$

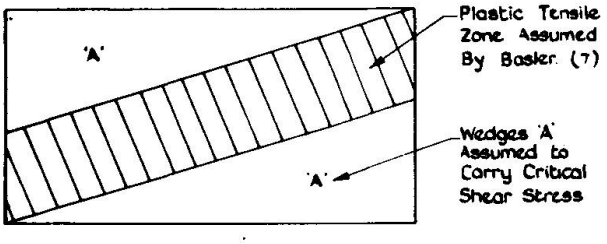

FIG. 2(a) COLLAPSE MODE ASSUMED IN BASLER THEORY.

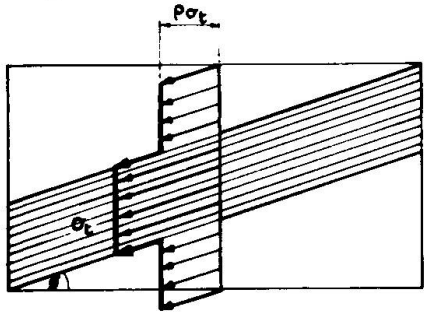

FIG. 2(b) MODIFIED BASLER TENSION FIELD MODEL ADOPTED BY OSTOPENKO; ρ = ½ TAKEN AS A TYPICAL VALUE

The results of this most interesting and valuable work have been used as the basis of the current design procedures used in the U.S.A. (10). However, it will be shown later in the present paper that the collapse model assumed by Basler is not correct and that it can result in both unduly conservative (safe) and understrength structures.

At the Conference of Steel Bridges (11), held in London in 1968 and later at the I.A.B.S.E. Conference (12) held in New York, the authors of the present paper presented the results of tests on 24 model girders, and showed that failure occurred when the girders

developed the collapse mechanism shown in Figure 3; the web yielding throughout the diagonal strip together with the development of

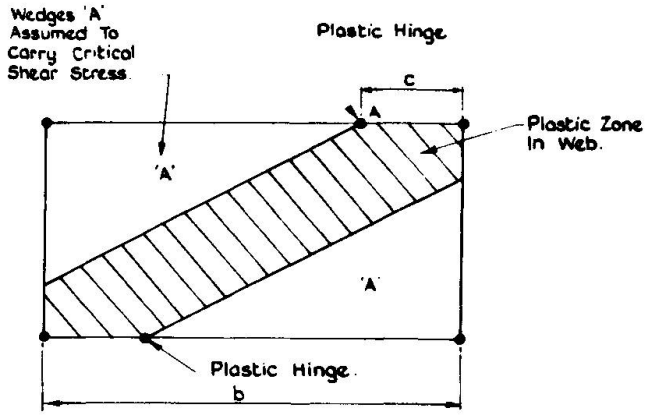

FIG 3(a) COLLAPSE MODEL PROPOSED BY ROCKEY & SKALOUD (12)

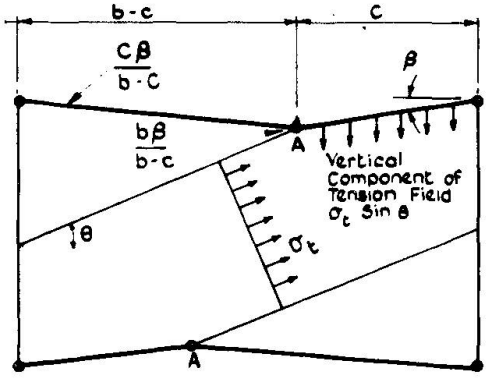

FIG 3(b) BEAM MECHANISM ASSUMED IN PROPOSED ROCKEY AND SKALOUD METHOD

plastic hinges in the flanges. It was also noted that the position of these plastic hinges varied with the flexibility of the flanges; with increasing flange stiffness the position of the plastic hinge (Q) moving towards the mid span position.

Figure 4 shows the possible modes of failure which can occur. In particular it is of interest to note that if the diagonal tension

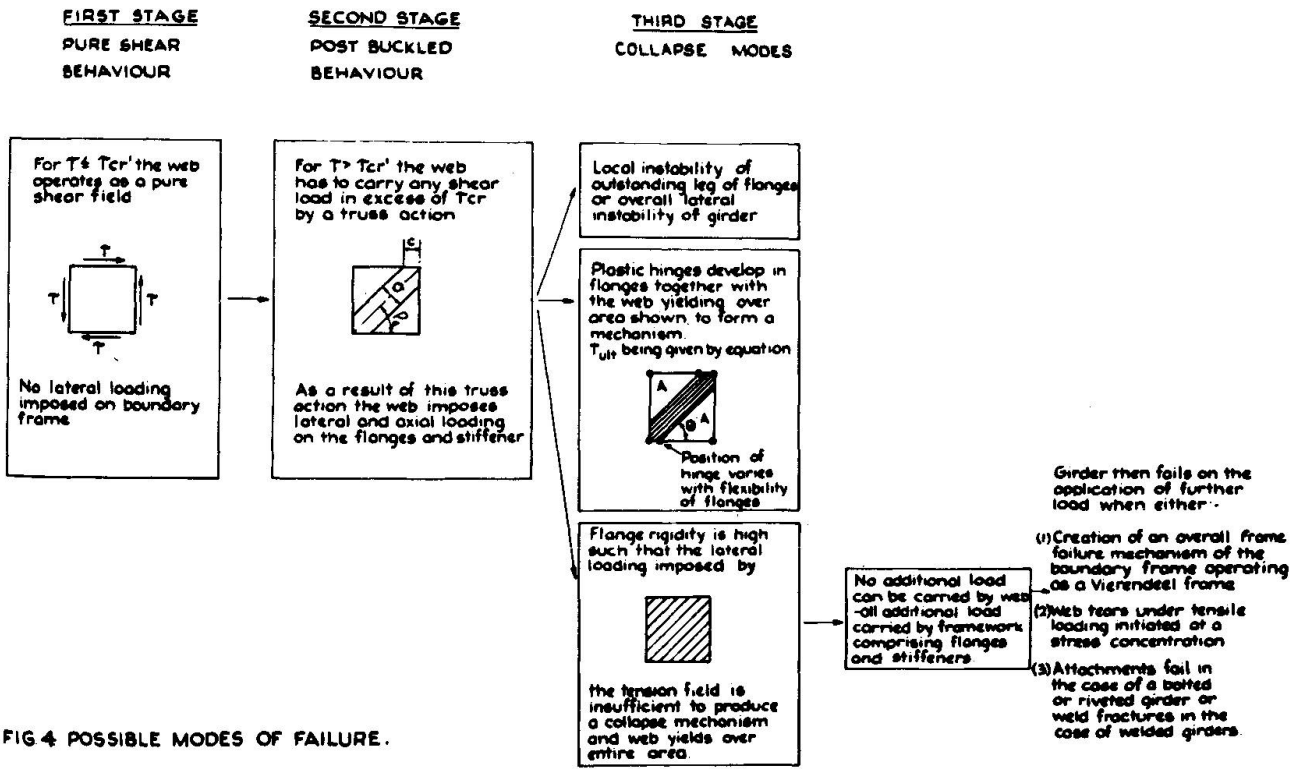

FIG 4 POSSIBLE MODES OF FAILURE.

loading is insufficient to develop plastic hinges in the flanges, then after the web has yielded any additional load has to be carried by the boundary framework, comprising the flanges and the stiffeners, acting as a Vierendeel girder.

At the same I.A.B.S.E. Conference, Fujii (13) presented a paper in which he presented a modification of Basler's theory. This modified theory involves the development of plastic hinges at mid span of the panel together with hinges over the stiffeners. It will be shown later that the modified model as proposed by Fujii, although recognising the part played by the flanges in the collapse of the girder, does not take into account the influence of the flange stiffness upon the position of the plastic hinge, and, therefore, Fujii's model is unable to deal with all of the failure modes and consequently gives results less satisfactory than the model proposed by the authors.

In August, 1969, Chern and Ostapenko (14) presented a new version of the Basler Collapse Mechanism. The model assumed by Chern and Ostapenko was similar to that assumed by Basler except for the fact that they allowed for the variation in σ_t across the section, see Figure 2(b). Furthermore, Ostapenko and Chern suggested that it would be more appropriate to use the value of τ_{cr} corresponding to the condition of the two edges supported by the flanges being clamped and the transverse edges being simply supported. They also discussed the value of ρ to be assumed in the modified tension field model, suggesting that for Practical Girders ρ should be taken as 0.5. Clearly if $\rho = 1.0$, then one would have the effect of a full tension field. It is this arbitrary choice in ρ and the fact that their tension band σ is still identical with Basler's so not allowing for the effect of flange rigidity which is the weakness in the Chern and Ostapenko approach, but with the influence of the flange flexibility parameter being clarified by the authors' present study; then as suggested by Chern and Ostapenko their model could be improved.

Chern and Ostapenko drew special attention to the frame action which occurs when the web yields and suggested a simple procedure to determine the magnitude of load required to produce this simple Vierendeel frame action.

2. EXPERIMENTAL INVESTIGATION

The experimental studies reported by the authors comprise three test series; series I and II dealing with the tests conducted by the authors and series III dealing with earlier tests made by one of the authors (15). The design details of the girders tested are given in Figure 5 and a summary of the dimensions of the girders and

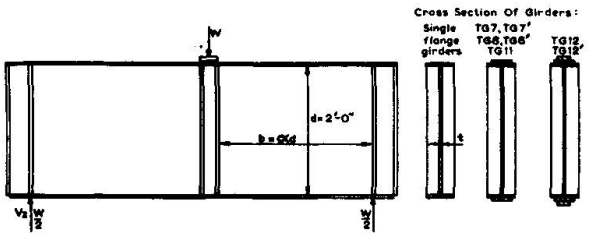

FIG. 5a. DETAILS OF SERIES I GIRDERS

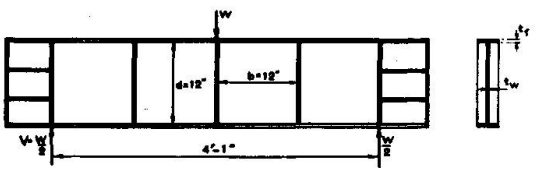

FIG. 5b. DETAILS OF SERIES II GIRDERS.

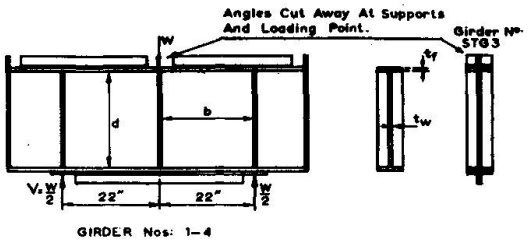

GIRDER Nos: 1–4

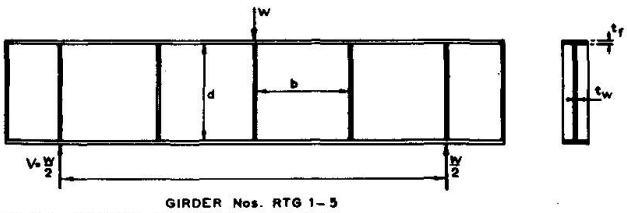

GIRDER Nos. RTG 1–5

FIG. 5c. DETAILS OF SERIES III GIRDERS.

the test data is given in Tables 1 - 3. It is beyond the scope of this paper to give a report on the testing procedure, and a full discussion of the test data obtained from these tests, but this information is available in reference (16).

2.1. DISCUSSION OF THE TEST RESULTS

Series I Girders

Table I gives the ultimate loads obtained from the 24 series I girders. Now since for each of the panel ratios examined, only the flexural stiffness of the flanges varied, the influence of flange stiffness upon the ultimate load carrying capacity of the girders is clearly demonstrated. It will be observed that the ultimate shear stress increases with the flange stiffness parameter ($I/_b{}^3{}_t$) until it reaches the shear yield stress indicating that the web has yielded over its complete surface.

Girder TG1 was very well instrumented, an electrical resistance strain gauge being attached at regular intervals along the flanges and demec gauge points placed across the compression diagonal of each of the web panels. Figure 6 shows the bending strains which were developed in the compression flange of girder TG1. It is of interest to note that at an applied load of 22.5 tons little bending of the flange had occurred but that after increasing to the ultimate load of 23.5 tons and then unloading there is a considerable plastic residue indicative of a plastic hinge having been developed. In the case of Panel W2 of Girder TG1, this plastic hinge is seen to have occurred at a distance of 0.25d. from the end stiffeners.

TABLE 1

Series I Girders. Aspect Ratio b/d = 1 b = 24in. d = 24in.

Girder No	Web Thickness t (in)	Flange* Dimensions in x in	$I/_b{}^3{}_t$ Units of 10^{-6}	W_{exp} Tons	% Gain Over Minimum Value Obtained with that Aspect Ratio	W_B Tons	W_{exp}/W_B
TG 1	0.107	4 x 0.185	1.47	22.6	0	34.26	1.43
TG 1[1]	0.107	4 x 0.187	1.47	24	6	32.63	1.36
TG 2	0.107	4 x 0.258	3.5	25.2	11.5	32.44	1.29
TG 2[1]	0.107	4 x 0.253	3.5	23.5	4	33.08	1.41
TG 3	0.108	4 x 0.495	27.9	28.5	26	34.48	1.21
TG 3[1]	0.108	4 x 0.497	27.9	27	19.5	32.25	1.19
TG 4	0.107	4 x 0.625	54.5	31.8	41	31.35	0.986
TG 4[1]	0.107	4 x 0.623	54.5	30.3	34	34.90	1.15
TG 13	0.103	4 x 0.997	224	41.7	84	34.66	0.831
Series I Girders. Aspect Ratio b/d = 1.5 b = 36in. d = 24in.							
TG 5[1]	0.103	8 x 0.375	7.35	23.4	0	29.22	1.12
TG 5	0.103	8 x 0.374	7.35	26.0	11	27.39	1.17
TG 6	0.103	8 x 0.644	34	28.4	21	30.55	1.07
TG 6[1]	0.103	8 x 0.635	34	26.7	14	26.43	0.99
TG 7	0.103	8 x 0.644 and 7 x 0.376	129	35.5	52	29.59	0.833
TG 7[1]	0.103	8 x 0.637 and 7 x 0.380	129	38.6	65	30.96	0.802
TG 8	0.103	8 x 0.639 and 7 x 0.62	254	40.3	72.5	30.44	0.755
TG 8[1]	0.103	8 x 0.644 and 7 x 0.634	254	41.4	76.5	30.41	0.735
Series I Girders. Aspect Ratio b/d = 2.0							
TG 9[1]	0.103	8 x 0.388	3.1	24.05	0	23.36	0.951
TG 9	0.103	8 x 0.388	3.1	24.55	2	25.0	1.04
TG 10	0.103	8 x 0.640	14.3	25.7	77	23.31	0.907
TG 11*	0.103	8 x 0.640 and 6 x 0.625	98.4	35.5	47.5	25.44	0.717
TG 12	0.103	9 x 0.780 and 8 x 0.62 and 7 x 0.489	384	45.7	90	23.22	0.508
TG 12[1]	0.103	9 x 0.767 and 8 x 0.63 and 7 x 0.501	384	49.2	104	24.00	0.488
Series I Girders. Aspect Ratio b/d = 0.79 b = 19in. d = 24in.							
TG 0	0.057	4 x 0.254	13.4				

* TG 11 had a depth d of 24.25".

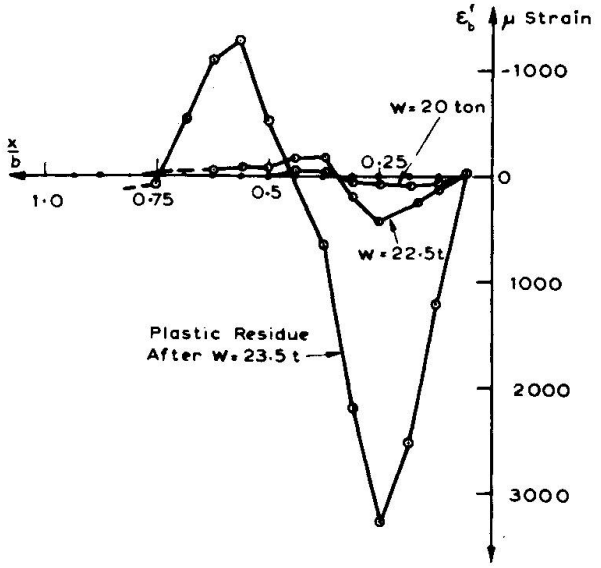

FIG. 6. COMPRESSION FLANGE BENDING STRAINS. GIRDER TG1 - PANEL W2.

Figure 7 shows the residual web deflections remaining in panel W1 after failure together with the diagonal mid plate tensile strains, acting across the diagonal AB which were measured at various loads. It is important to note that the wave inclination is along the diagonal and that the web strains are also reasonably symmetric about the diagonal since Basler, in the model shown in Figure 2, has assumed a different model.

It is also of interest to note that at an applied load of 20 tons which was 83.5% of the failure load, the diagonal membrane stresses are still elastic.

Figure 8 shows girder TG4 after it had been tested to failure, whilst Figure 9 gives the plastic residual deformations in the flanges and the residual diagonal membrane strains in the webs.

In the case of panel W1 it is seen that the plastic hinge is now 0.405 d from the end stiffener. Thus we see that as a result of increasing the flexural rigidity of the flange, the position of the hinge has moved closer to the mid section of the panel. The variation of the position of the hinge in the compression flange with the I/b^3t parameter has been plotted in Figure 10 from which it will be noted that as $I/b^3t \to \infty$ so the c/b ratio approaches 0.5. It will be noted from Figure 11 that if a residual strain of 1000 micro-strain is taken to indicate full plasticity, then the width of the fully yielded diagonal tensile band intercepts close to the position of the plastic hinges which have developed in the flanges, thus showing that the plastic collapse model proposed, see Figures 3 and 4, is completely realistic. Referring to Figure 9, it will be noted that the collapse mechanism is similar to that shown in Figure 12(a), with a plastic hinge developed at all corners. However, it should be appreciated that when the web collapses the framework develops a Vierendeel Mechanism as shown in Figure 12(b). It is clear that on combining Figures 12(a) and 12(b) one achieves the Mechanism obtained in Figure 12(c), which is of the same form as that given in Figure 9.

The series I test programme had established the basis of the design method but it was desirable that further tests be conducted on multi-bay girders to study the influence of panel continuity and to obtain data from girders having different depth/thickness ratios. With these two factors in mind the test girders comprising the Series II programme were designed, for details see Figure 5 and Tables 2 and 3. Two web thicknesses were chosen, the depth/thickness of the thickest plate giving a high buckling stress whereas the thinner plate provided web panels in which the critical load was sufficiently low to ensure that the post buckled action dominated; the buckling shear stresses for the square panels, assuming simply supported edges, being 1.13 and 5 tons/in^2 respectively. The test data obtained from this test programme was most useful in confirming and extending the basis of the theory which resulted from Series I study. Figure 13 compares the residual contour plots which were obtained in a panel of girder TG15 with that occurring in a panel of girder TG19. It will be noted from Table 2 that Girders TG15 and 19 were similar in all respects except for the thickness of the flange members. It will be seen that in the case of girder TG19, the web had developed a uniform tension field, consisting of 8 half waves which covered the whole web, whereas in the case of TG15 a less well defined

TABLE 2

Series II Girders. All panels of Aspect Ratio b/d = 1.0 b = 12m d = 12in.

Girder No	Web Thickness t (in)	Flange Dimensions in x in	I/b^3t Units of 10^{-6}	Type of Failure	$\frac{c}{b}$ exp	$\frac{c}{b}$ th	W_{exp} Tons	W_{RS} Tons	$\frac{\tau_{cr}}{\tau_y}$	$\frac{\tau_{ult}}{\tau_y}$	$\frac{\tau_{exp}}{\tau_{yw}}$	$\frac{V_B}{V_{exp}}$	$\frac{V_{RS}}{V_{exp}}$
TG 14	0.038	3 x 0.123	7.4	Mechanism, Figure 4	0.23	0.316	5.09	4.63	0.138	0.619	0.681	0.978	0.910
TG 15	0.038	3 x 0.197	23.5	Mechanism, Figure 4	0.35	0.418	5.89	5.78	0.138	0.773	0.788	0.845	0.982
TG 16	0.038	3 x 0.254	60.2	Mechanism, Figure 4	0.488	0.50	6.28	6.72	0.138	0.899	0.840	0.793	1.07
TG 17*	0.038	3 x 0.367	190	Mechanism, Figure 4	0.467	0.50	7.82	6.72	0.138	0.899	1.045	0.637	0.859*
TG 18*	0.038	3 x 0.510	471	Web has yielded, Frame Mechanism	0.50	0.50	10.10	6.72	0.138	0.899	1.35	0.493	0.665*
TG 19	0.038	3 x 0.611	835	" " " "	0.50	0.50	10.9	6.72	0.138	0.899		0.456	
TG 20	0.08	3 x 0.128	3.35	Premature Failure Flange Collapse due to Bending Stress > σ_{yf}		0.168	10.23	11.63	0.576	0.710	0.624	1.34	1.14
TG 21	0.08	3 x 0.192	11.9	Mechanism, Figure 4	0.296	0.269	14.25	12.95	0.576	0.790	0.870	0.961	0.909
TG 22	0.08	3 x 0.255	29.3	Mechanism, Figure 4	0.367	0.457	15.8	15.38	0.576	0.939	0.964	0.866	0.974
TG 23	0.08	3 x 0.363	95.2	Mechanism, Figure 4	0.484	0.50	16.3	15.95	0.576	0.973	0.995	0.840	0.978
TG 24*	0.08	3 x 0.510	236.4	Web has Yielded, Frame Mechanism	0.50	0.50	19.3	15.95	0.576	0.973	1.18	0.709	0.826*
TG 25*	0.08	3 x 0.612	408.6	" " " "	0.5	0.5	20.8	15.95	0.576	0.973	1.27	0.658	0.766*

* For these Girders $\tau_{exp}/\tau_{yw} > 1$ ∴ Frame Mechanism involved

TABLE 3

SERIES III GIRDERS

Girder No	Aspect Ratio	Web Thickness t in.	Web depth d in.	Web width b in.	Flange Dimen. in. x in. *	Girder No	Type of Failure	W_{exp} Tons	$\frac{\tau_{cr}}{\tau_{yw}}$	$\frac{\tau_{ult}}{\tau_{yw}}$	$\frac{\tau_{exp}}{\tau_{yw}}$
STG 1	1.85	0.079	11	21.7	5 x 0.312	STG 1	Mechanism Figure 4	12.0	0.445	0.834	0.771
STG 2	1.98	0.063	9.95	19.75	5 x 0.25	STG 2	" " 4	7.9	0.304	0.743	0.627
STG 3	1.98	0.056	10	19.8	5 x 0.187 plus 2½"x2½"x5/16" Angles.	STG 3	Fully developed tension field, frame mechanism.	20.0	0.251	0.814	> 1.0
STG 4	1.98	0.049	9.9	19.60	4 x 0.250	STG 4	Mechanism Figure 4	7.0	0.206	0.590	0.786
RTG 1	1.0	0.05	12	12	3 x 0.177	RTG 1	Mechanism Figure 4	8.0	0.215	0.578	0.730
RTG 2	1.0	0.05	12	12	3 x 0.183	RTG 2	" " 4	8.15	0.215	0.586	0.744
RTG 3	1.0	0.0375	12	12	3 x 0.183	RTG 3	" " 4	4.85	0.164	0.709	0.667
RTG 4	1.0	0.0375	10	10	3 x 0.183	RTG 4	" " 4	11.7	0.378	0.610	0.808
RTG 5	0.94	0.064	11.7	11	3 x 0.187						

Tension Field consisting of only 3 half waves had been developed. In the case of girder TG19 the tensile forces imposed by the membrane field upon the boundary members had been insufficient to develop plastic hinges in the flanges, thus the web was able to develop the full diagonal tension action.

In such cases there are two distinct phases; in the first phase the post buckled behaviour develops until the web has yielded over its complete surface, the flange remaining elastic. Once this stage has been reached additional shear load can only be carried by the framework and failure will result when the framework, comprising the flanges and the stiffeners, acting like a Vierendeel Frame, develops sufficient hinges to form a mechanism, such as that shown in Figure 12(c).

An alternative failure is encountered in aluminium girders when, because of the materials reduced ductibility under the tensile strains. Figure 14 shows a typical aluminium girder with very stiff flanges, which has experienced a tensile failure in the web.

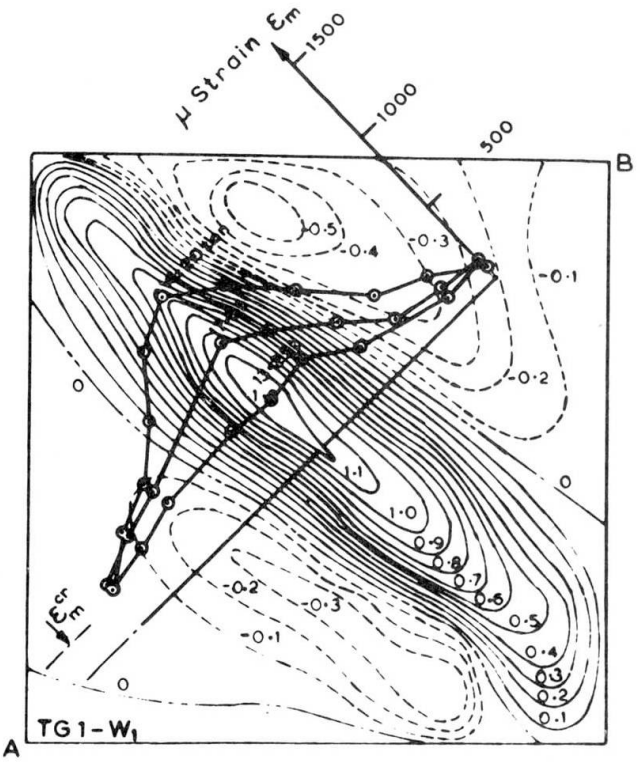

FIG.7. Tensile strains developed across diagonal AB of panel W1 in girder TG1 together with the residual web deflections which remained after failure.

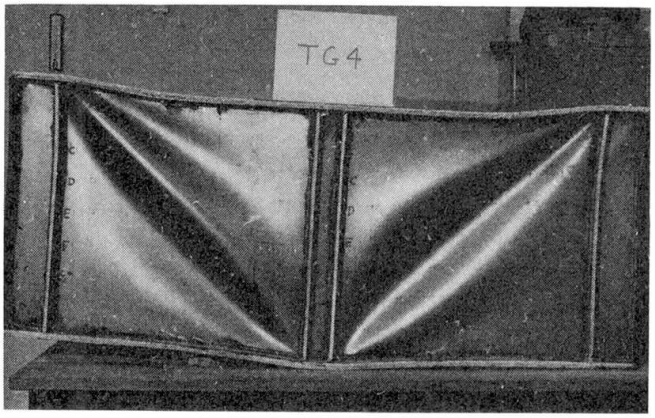

FIG.8. Girder TG4 after test to failure. Note well developed hinges.

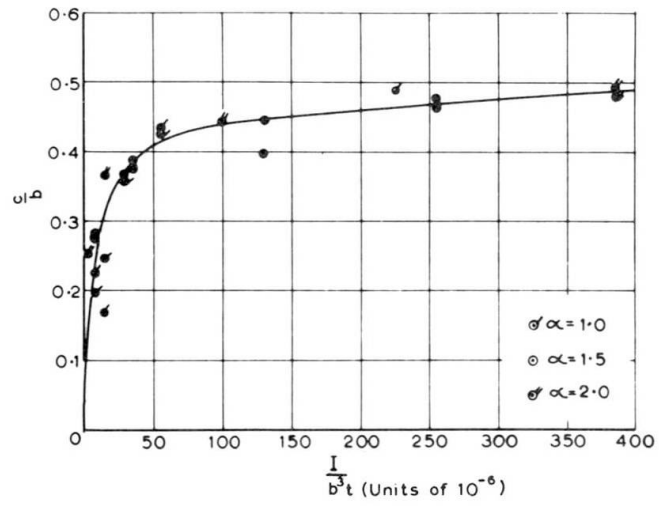

FIG.10. VARIATION OF THE POSITION OF THE PLASTIC HINGE REPRESENTED BY THE PARAMETER c/b, AND THE FLANGE FLEXIBILITY PARAMETER (I/b^3t).

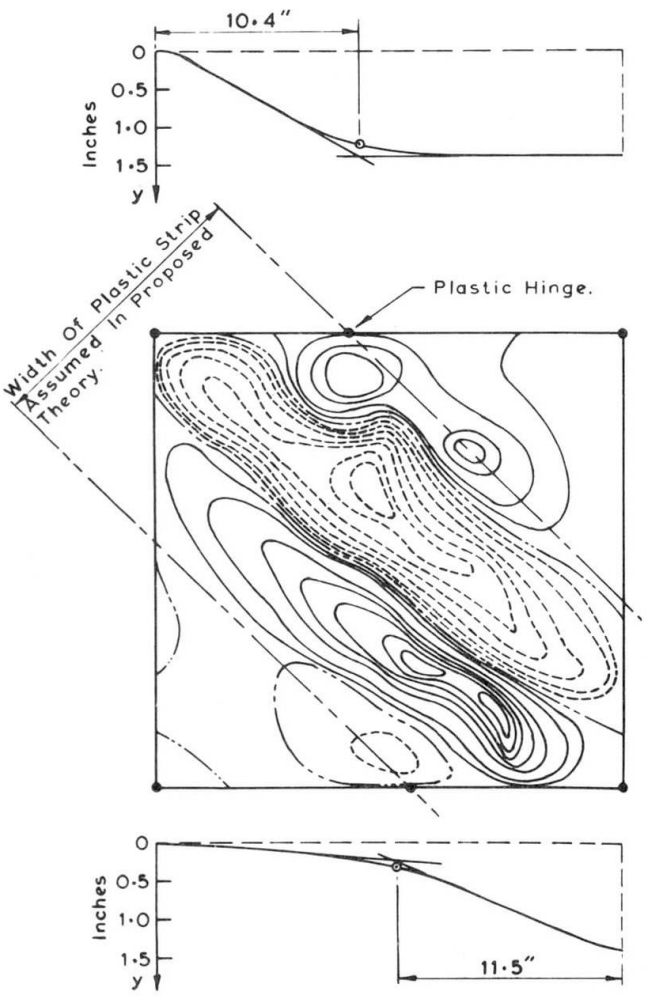

FIG.9. RESIDUAL DEFORMATIONS IN FLANGES AND WEB OF PANEL W1 OF GIRDER TG4 (Series I)

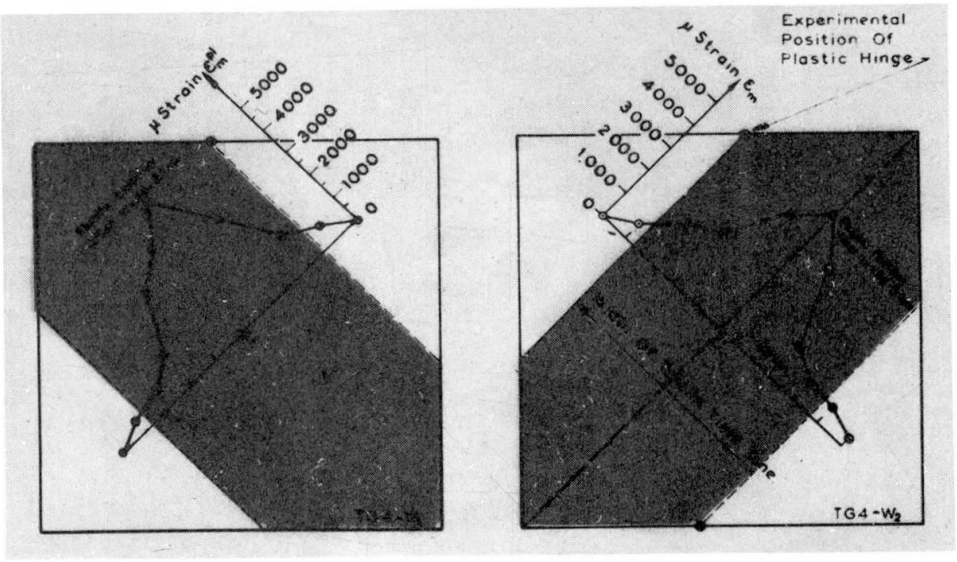

FIG. 11. RESIDUAL DIAGONAL MEMBRANE STRAINS – PANELS W_1 & W_2 OF GIRDER TG4.

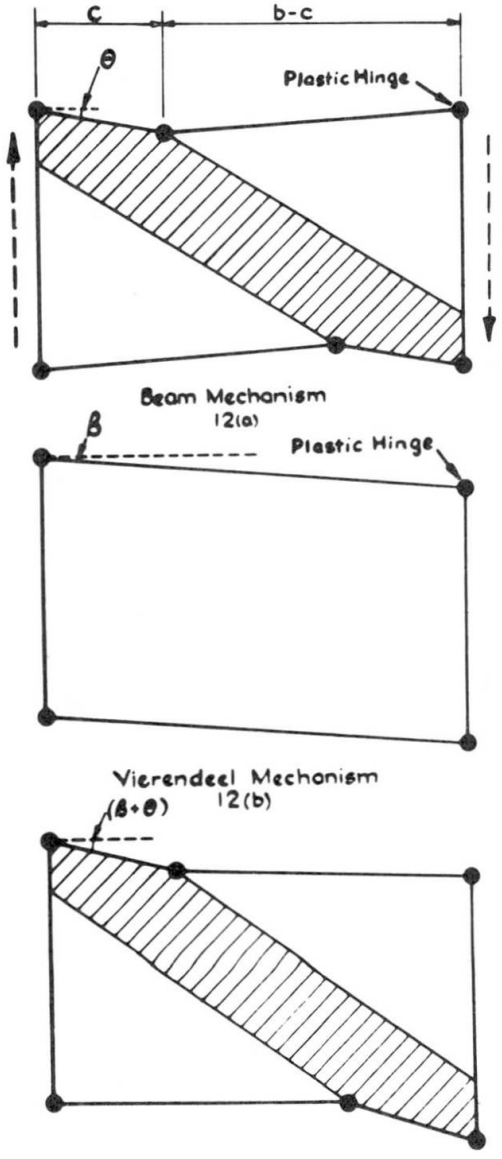

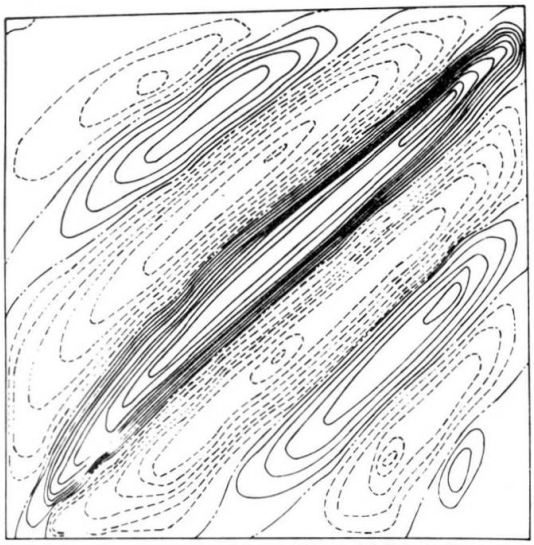

FIG. 13(a) RESIDUAL CONTOUR PLOT OF GIRDER TG 19. FLANGES VERY STRONG – WEB DEVELOPS FULL SHEAR STRENGTH.

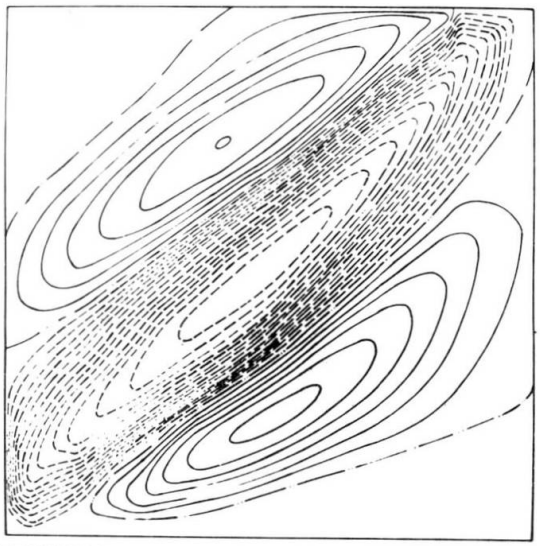

FIG. 13(b) RESIDUAL CONTOUR PLOT OF A PANEL ON GIRDER TG 15

Figures 11, 20, 22 and 24 are examples of the possible modes of failure which can be encountered in a webplate subjected to shear as shown in Figure 14.

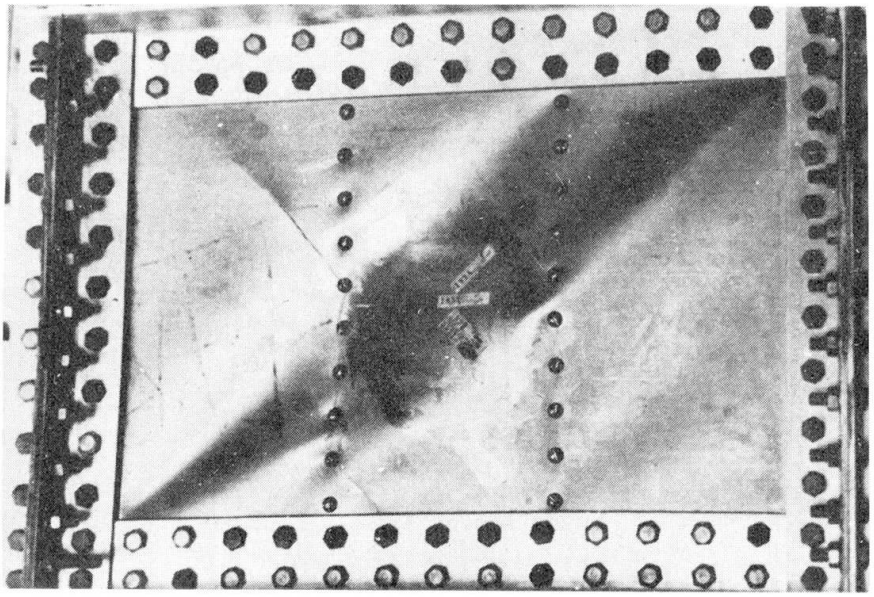

3. DESIGN CONCEPT

3.1. Introduction

The research study has shown that the behaviour of a plate girder web can be divided into three stages.

Stages I and II

In Stage I, which only applies to a perfectly flat plate, for shear stresses less than the critical buckling stress the web panels carry the applied load by a pure shear action.

The second mode of action results from the fact that in a buckled web the compressive stresses cannot increase and any additional load has to be carried by a tensile truss action. As illustrated in the preceding sections the post buckled action of a web plate is influenced by the flexural stiffness of the flanges and stiffeners; with very stiff flanges the tensile field action is uniformly distributed across the webplate, whereas with more flexible flanges the tensile field action is restricted to a diagonal band.

With normal welded plate girders which have webs with significant permanent deformations, no buckling phenomena will be observed and the loadings which are associated with Stage II occur as soon as a load is applied to the girder.

Failure occurs when the diagonal tension band, see Figure 3, yields and the boundary members develop sufficient plastic hinges to result in a failure characterised by one of the three possible forms of failure listed under Stage III, see also Figure 4.

Stage III

(a) If the lateral membrane loading on the flange is sufficient to develop plastic hinges in the flanges, then failure will be due to the development of a yielded diagonal strip together with plastic hinges in the tension and compression flanges; see Figures 3 and 4.

(b) If, however, the membrane loading corresponding to a

yielded web is not sufficient to develop plastic hinges in the flanges, then failure will occur when either :-

(1) the web material fractures, such as occurs in an aluminium web, see Figure 14, which shows a typical diagonal web fracture

(2) the frame work comprising the flanges and the stiffeners develop a 'frame' mechanism as a result of carrying further loading as a framework since the fully yielded web cannot carry any additional shear load ; see Figure 12.

(3) a third class of failure which can occur is when the compression flange buckles laterally or torsionally, or develops a local buckle in the outstanding flange of the flanges.

3.2. THEORETICAL BASIS

STAGE 1

For an initially plane web, for loading below the buckling stress, τ_{cr}, the stress state is assumed to be one of pure shear. Obviously the value of τ_{cr} will vary with the torsional rigidity of both the flanges, and the stiffeners.

Following buckling, the web is unable to withstand any further compression loading and any additional loading has to be carried by a tension field action. The present solution does not attempt to deal with the very complicated stress field which occurs in the elastic post buckled range, being solely concerned with the final collapse mode. Observations of the collapse behaviour of girders indicates that the stress and deflection distributions vary quite rapidly and significantly at loads close to the ultimate.

As shown earlier, the experimental evidence resulting from the present study is that at collapse the web develops a tension band as shown in Figure 3 in which the angle of the tension band is equal to the inclination of the geometrical diagonal and that the tension band is symmetric with respect to the geometric diagonal. The width of the diagonal tension load is assumed to be such that at its junction with the flange its edges coincide with position of the plastic hinge in the flanges. The above assumptions with respect to the inclination of the diagonal tension field will clearly result in lower bound solutions for values of $\alpha > 1$ when the flanges are stiff.

The position of the plastic hinge in the flange may be theoretically determined using the collapse mechanism shown in Figure 3(b). This mechanism assumes that the hinge coincides with the edge of the diagonal strip and that the loading consists of the vertical component of the diagonal tensile membrane stress $\sigma_t{}^y$. The solution of this simple mechanism reduces to the solution of the following cubic equation given in equation 3.

$$\left(\frac{c}{b}\right)^3 - \left(\frac{c}{b}\right)^2 + \frac{4\, z_f \sigma_{yf}}{b^2 t\, \sin^2\theta\, (\sigma_t{}^y)} = 0 \qquad \ldots\ldots\ldots\ldots (3)$$

where z_f denotes the plastic modulus for flange assembly. From a study of all experimental data from the technical literature it is

proposed that when the web buckling stress τ_{cr} is less than half the shear yield stress τ_{yw} a depth of web plate, d_e, as obtained from equation 4 be assumed to act with the flange.

$$d_e = 30(1 - \frac{2\tau_{cr}}{\tau_{yw}})t \qquad \ldots\ldots\ldots\ldots\ldots\ldots(4)$$

Thus we see that there are two stress regions, see Figures 3 and 15.

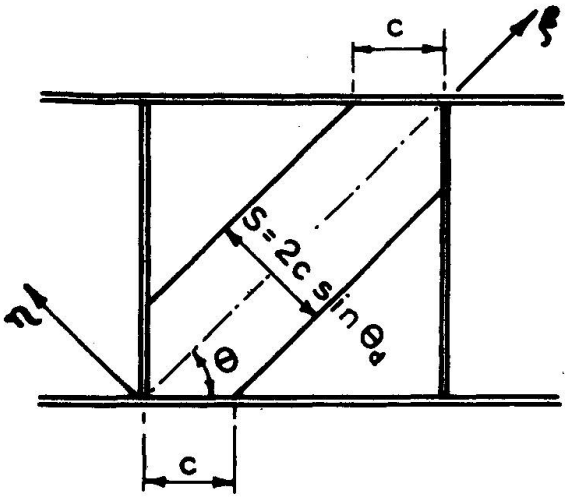

FIG. 15.

(1) two triangular wedges in which the critical shear stress is assumed to act

(2) a yielded diagonal strip

The tension stress σ_t is assumed to act uniformly over the diagonal band, yielding occurring when σ_t reaches a value σ_t^y.

The stress condition, see Figure 15, in the diagonal web strip, is given by :-

$$\sigma_\zeta = \tau_{cr} \text{ Sin } 2\theta + \sigma_t^y$$

$$\sigma_\eta = \tau_{cr} \text{ Sin } 2\theta \qquad \ldots\ldots\ldots(5)$$

$$\tau = \tau_{cr} \text{ Cos } 2\theta$$

Using the Huber Von Mises plasticity condition, the material yields when $\sigma_{mc} = \sigma_{yw}$ where

$$\sigma_{mc} = \sqrt{\sigma_\zeta^2 + \sigma_\eta^2 - \sigma_\zeta\sigma_\eta + 3\tau^2} \qquad \ldots\ldots\ldots\ldots(6)$$

Substituting equation 5 into 6 and rearranging yields

$$\sigma_t^y = -\frac{3}{2}\tau_{cr} \text{ Sin } 2\theta + \sqrt{\sigma_{yw}^2 + \tau_{cr}^2\left(\left(\frac{3}{2} \text{ Sin } 2\theta\right)^2 - 3\right)} \qquad \ldots\ldots\ldots\ldots(7)$$

The diagonal membrane tensile force will develop axial forces in both the stiffeners and the flanges, see equations 9 and 12 in the Authors' Reports (16).

The shear force V_σ carried by the diagonal strip

= width of strip x web thickness x σ_t^y x Sinθ

$$V_\sigma = 2ct \text{ Sin}^2\theta\left(-\frac{3}{2}\tau_{cr}\text{Sin}2\theta + \sqrt{\sigma_{yw}^2 + \tau_{cr}^2\left(\left(\frac{3}{2}\text{Sin}2\theta\right)^2 - 3\right)}\right) \qquad \ldots\ldots\ldots(8)$$

The total shear force $V_{ult} = V_\sigma +$ the shear force V_{cr} necessary to cause the plate to buckle.

$$V_{ult} = V_{cr} + V_\sigma = \tau_{cr}\, dt + 2ct \text{ Sin}^2\theta\left(-\frac{3}{2}\tau_{cr} \text{ Sin } 2\theta + \right.$$

$$\sqrt{\sigma_{yw}^2 + \tau_{cr}^2\left(\left(\frac{3}{2}\ \mathrm{Sin}\ 2\theta\right)^2 - 3\right)} \qquad \ldots\ldots\ldots (9)$$

and the corresponding shear stress τ_{ult} is given by

$$\tau_{ult} = \tau_{cr} + \frac{2c}{d}\ \mathrm{Sin}^2\theta\left(-\frac{3}{2}\ \tau_{cr}\ \mathrm{Sin}\ 2\theta + \sqrt{\sigma_{yw}^2 + \tau_{cr}^2\left(\left(\frac{3}{2}\ \mathrm{Sin}\ 2\theta\right)^2 - 3\right)}\right) \qquad \ldots\ldots\ldots (10)$$

The value of τ_{cr} depends on the tensile rigidity of the flanges. It is recommended that with conventional plate girders having single flat flange plates, it can be assumed that the web is simply supported along all 4 edges. However, should the flanges be of tubular construction it would be more appropriate to assume the web is clamped to the flanges and simply supported at the vertical stiffeners.

$$\text{Now} \quad \tau_{yw} = \sigma_{yw}/\sqrt{3}$$

Therefore, dividing equation 10 by τ_{yw} one obtains

$$\frac{\tau_{ult}}{\tau_{yw}} = \frac{\tau_{cr}}{\tau_{yw}} + 2\sqrt{3}\ \frac{c\alpha}{b}\ \mathrm{Sin}^2\theta\left(-\frac{\sqrt{3}}{2}\ \mathrm{Sin}\ 2\theta\left(\frac{\tau_{cr}}{\tau_{yw}}\right) + \sqrt{1 + \left(\frac{\tau_{cr}}{\tau_{yw}}\right)^2\left(\frac{3}{4}\ \mathrm{Sin}^2(2\theta) - 1\right)}\right) \qquad \ldots\ldots\ldots (12)$$

It is of interest to consider how equation (12) satisfies the following limiting conditions.

(1) Very Thin Webs and Rigid Flanges

For very thin webs $\tau_{cr} \to 0$, in which case

$$\frac{\tau_{ult}}{\tau_{yw}} = 2\sqrt{3\alpha}\ \frac{c}{b}\ \mathrm{Sin}^2\theta$$

Since for rigid flanges, $\frac{c}{b} = 0.5$, then for square web panels in which $\theta = \frac{\pi}{4}$ one obtains the value for τ_{ult} of :-

$$\frac{\sqrt{3}}{2}\ \tau_{yw} \quad \text{or} \quad \frac{\sigma_{yw}}{2}$$

which agrees with the value obtained from Wagner's Theory for a complete tension field.

(2) Very Thick Webs

When webs are very thick, then $\tau_{cr} \to \tau_{yw}$ and the terms inside the main brackets reduces to zero so that equation (12) reduces to $\tau_{ult} = \tau_{cr}$; which again is as to be expected.

(3) Very Flexible Flanges

Finally, if $\frac{c}{b} \to 0$, as would be the case if the flanges had

zero stiffness, then

$$\tau_{ult} = \tau_{cr}$$

Thus we would see that equation (12) satisfies the extreme boundary conditions exactly.

When $\sqrt{3}\,\tau_{cr}$ exceeds the limit of proportional stress of the material then the effective modulus E_r is less than the modulus of Elasticity E. This reduces the critical shear stress; and to allow for this Basler and his colleagues have recommended that τ_{cr} be replaced by τ_{cre} when $\tau_{cr} \quad \frac{0.8\,y}{\sqrt{3}}$, τ_{cre} being obtained from equation 18.

$$\frac{\tau_{cre}}{\tau_{yw}} = 1 - \frac{0.16\tau_{yw}}{\tau_{cr}}$$

Using equation (13), the relationship between the ratio τ_{ult}/τ_{yw} and the depth to thickness ratio for different values of c/b have been plotted in Figure 16 for the case of a square web plate. The values of τ_{ult}/τ_{yw} as derived from Basler's ultimate load expression, equation 2, have also been plotted using the same relationship between τ_{cre}, τ_{cr} and τ_{yw}, and it is clearly seen that for very flexible flanges Basler's equation over-estimates the strength of the girder and for relatively stiff flanges it underestimates the strength, this being particularly true for the larger values of α.

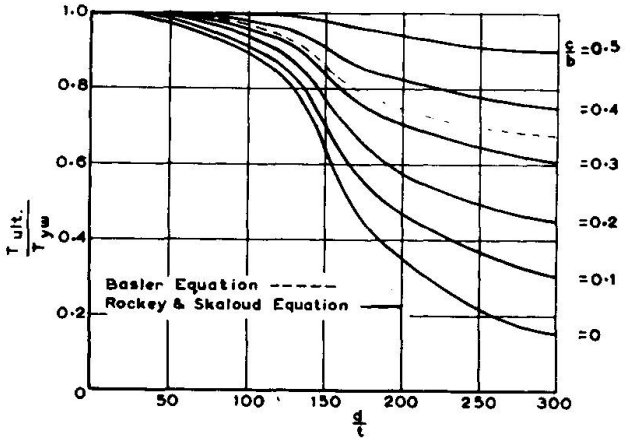

FIG. 16.

4.0. DISCUSSION OF TEST RESULTS

COMPARISON OF DESIGN PROCEDURE WITH EXPERIMENTAL DATA

In this section, the ultimate load method of design developed in the previous section will be checked against all the available experimental data.

In these tables, V_{RS} is the ultimate shear load obtained by the authors when using equation (14) together with equation (19) when $T_{cr}/T_{yw} > 0.5$.

In Tables 1 - 6, the ultimate loads predicted by the authors' Method has been compared with the experimental failure loads and the theoretical values predicted by Basler (6), Fujii (13) and Ostapenko (14).

$$\frac{T_{cre}}{T_{yw}} = 1 - 0.25\,\frac{T_{yw}}{T_{cr}} \qquad \text{.....(14)}$$

Unfortunately, it is not possible in the restricted space of the present article to refer in detail to all of the tests. However, a full discussion is available in Reference (16).

Table 2 presents the results obtained from the twelve Series II girders. These girders had web panels with an aspect ratio of one, the only variables being in the thickness of the flanges and the web material. It will be noted that for the thinner webs the predicted failure loads for girders TG14, 15 and 16 are very close to the actual failure load of the girders. With girders TG17 - 19 the flanges were thick and the web developed full plasticity without causing a plastic hinge in the flanges, failure occurring when the boundary members developed a frame mechanism. It will be noted that the τ_{exp}/τ_{yw} ratio for girders TG14 - 19 increases with an increase in flange thickness, until in the case of girders 17 - 19, it exceeds unity indicating that the web is fully yielded, and the girder is carrying the same load as a Vierendeel type structure.

In such cases the ultimate shear load is given by equation (20) in which V_f is the additional shear load necessary to cause the framework to fail a Vierendeel girder mechanism, see figure 13(c). Ignoring the presence of the yielded web but allowing for the reduction in the strength of the flanges due to the axial stresses set up in the flanges by the membrane field.

$$\text{Ultimate shear load} = V_{RS} + V_f$$

V_f can be readily determined using standard design methods for the plastic collapse of structures.

It will be noted that the proposed design procedure gives good agreement with the actual failure loads, see Tables 1 - 6.

TABLE 4

TEST DATA FROM REFERENCE 18 - SAKAI, DOI, NISHINO AND OKUMWA

GIRDER NO	$a = \frac{b}{d}$	$\frac{d}{t}$	WEB		FLANGES		V_{exp} Tons	$\frac{\tau_{exp}}{\tau_{yw}}$	V_{RS} Tons	$\frac{\tau_{cr}}{\tau_{yw}}$	$\frac{\tau_{ult}}{\tau_{yw}}$	$\frac{V_B}{V_{exp}}$	$\frac{V_F}{V_{exp}}$	$\frac{V_O}{V_{exp}}$	$\frac{V_{RS}}{V_{exp}}$
			$t \times b \times d$ mm x mm x mm	σ_{yw} Kg/mm²	$t_f \times B_f$ mm x mm	σ_{yf} Kg/mm²									
G1	2.61	55	8 x 1150 x 440	44	30 x 160	42	82	0.917	87.4	0.83	0.978	1.18	0.945	1.01	1.07
G2	2.61	55	8 x 1150 x 440	44	30 x 200	42	84	0.939	87.4	0.83	0.978	1.15	0.923	0.984	1.04
G3	2.63	60	8 x 1467 x 560	44	30 x 160	42	99	0.870	107.9	0.723	0.948	1.03	0.992	1.01	1.09
G4	3.57	70	8 x 2000 x 560	44	30 x 250	42	97	0.852	104.0	0.710	0.958	1.02	1.01	1.01	1.07
G5	2.68	70	8 x 1500 x 560	44	30 x 250	42	107	0.940	107.6	0.722	0.940	0.96	0.916	0.932	1.01
G6	1.25	70	8 x 687 x 560	44	30 x 250	42	120	1.05	112.9	0.795	0.997	0.94	0.820	0.892	0.941
G7	2.68	70	8 x 1500 x 560	44	30 x 250	42	107	0.940	107.6	0.722	0.946	0.95	0.920	0.892	1.01
G9	2.78	90	8 x 2000 x 720	44	30 x 250	42	118	0.806	117.9	0.538	0.805	0.835	1.054	0.838	0.999

It is of interest to note that Nishino and Okumwa in the discussion of their tests, write, "The plastic collapse loads increase with increase of flange area for the same web plate, whereas the theory of Basler predicts the same collapse; therefore, testing of girders with still heavier flanges may reveal the difference and lead to a clear conclusion".

It is because the design procedure proposed by the authors' of the present paper allows for the influence of flange stiffness upon the post buckled behaviour of the web, that it is capable of accurately predicting the failure load of the girders.

TABLE 5

TEST DATA FROM REFERENCE 19 - NISHINO AND OKUMMA

GIRDER NO	$a = \frac{b}{d}$	$\frac{d}{t}$	WEB $t \times b \times d$ mm x mm x mm	WEB σ_{yw} Kg/mm²	FLANGES $t_f \times B_f$ mm x mm	FLANGES σ_{yf} Kg/mm²	V_{exp} Kips	$\frac{\tau_{exp}}{\tau_{yw}}$	V_{RS} Kips	$\frac{\tau_{cr}}{\tau_y}$	$\frac{\tau_{ult}}{\tau_y}$	$\frac{V_B}{V_{exp}}$	$\frac{V_F}{V_{exp}}$	$\frac{V_O}{V_{exp}}$	$\frac{V_{RS}}{V_{exp}}$
G1	2.69	59.6	9.1 x 1450 x 543	38.0	22.4 x 301.0	44	110.5	1.02	105.8	0.826	0.976	0.904	1.06	1.02	0.958
G2	2.69	59.6	9.1 x 1450 x 543	38.0	22.4 x 220.0	44	104	0.959	105.8	0.826	0.976	0.961	0.925	1.10	1.02
G3	2.64	76.8	9.4 x 1900 x 722	38.0	22.2 x 302.0	44	124.5	0.836	134.5	0.712	0.903	1.04	1.02	1.19	1.08
G4	2.64	78.3	9.2 x 1900 x 720	38.0	22.1 x 243.0	44	114.5	0.788	126.1	0.701	0.868	1.10	-	-	1.10

TABLE 6

Test Data from Reference 20 - Longbotton and Heyman

GIRDER NO	$a = \frac{b}{d}$	$\frac{d}{t}$	WEB $t \times b \times d$ in x in x in	WEB σ_{yw} Tons/in²	FLANGES $t_f \times B_f$ in x in	FLANGES σ_{yf} Tons/in²	τ_{exp} Tons	W_{RS} Tons	$\frac{\tau_{cr}}{\tau_y}$	$\frac{\tau_{ult}}{\tau_y}$	$\frac{\tau_{exp}}{\tau_{yw}}$	$\frac{V_B}{V_{exp}}$	$\frac{V_{RS}}{V_{exp}}$
A1	1.28	94	0.056 x 6.78 x 5.25	16.7	0.25 x 1.0	18.6	5.76	5.64	0.774	0.990	1.02	0.880	0.975
A2	2.04	94	0.056 x 10.75 x 5.25	16.7	0.25 x 1.0	18.6	4.85	5.58	0.722	0.966	0.855	0.968	1.13
A4	2.1	85	0.056 x 10.0 x 4.75	16.7	0.25 x1.375	18.6	2.6	2.53	0.771	0.853	1.01	0.844	0.961

TABLE 7

TEST DATA FROM REFERENCE 9 - BASLER, YEN, MUELLER AND THURLIMANN

GIRDER NO	$a = \frac{b}{d}$	$\frac{d}{t}$	WEB $t \times b \times d$ in x in x in	WEB σ_{yw} Kips/in²	FLANGES $t_f \times B_f$ in x in	FLANGES σ_{yf} Kips/in²	$\frac{\sigma_b}{\sigma_b}$ exp	$\frac{\sigma_b}{\sigma_b}$ th	V_{exp} Kips	V_{RS} Kips	$\frac{\tau_{cr}}{\tau_y}$	$\frac{\tau_{ult}}{\tau_{yw}}$	$\frac{\tau_{exp}}{\tau_{yw}}$	$\frac{V_B}{V_{exp}}$	$\frac{V_F}{V_{exp}}$	$\frac{V_O}{V_{exp}}$	$\frac{V_{RS}}{V_{exp}}$
G6 T1	1.5	259	0.193 x 50 x 75	36.7	0.778 x 12.13	37.9	-	0.285	116	110.7	0.136	0.541	0.567	0.97	0.92	1.05	0.954
G6 T2	0.75	259	0.193 x 50 x 37.5	36.7	0.778 x 12.13	37.9	-	0.375	150	151.6	0.258	0.741	0.733	1.05	1.03	1.06	1.01
G6 T3	0.50	259	0.193 x 50 x 25	36.7	0.778 x 12.13	37.9	-	0.500	177	184.2	0.484	0.901	0.866	1.02	1.00	1.08	1.04
G7 T1	1.0	255	0.196 x 50 x 50	36.7	0.769 x 12.19	37.6	0.33	0.33	140	137.5	0.184	0.661	0.674	1.01	0.95	1.04	0.981
G7 T2	1.0	255	0.196 x 50 x 50	36.7	0.769 x 12.19	37.6	0.33	0.33	145	137.3	0.184	0.661	0.674	0.98	0.90	1.00	0.947

The very extensive tests conducted by Basler, Yen, Mueller and Thurlimann (9) at Lehigh have provided test data for deep girders having web depths of 50" the maximum web thickness being only 3/16". The girders thus had a comparatively high depth/thickness ratio and since the aspect ratio of the web panels varied from 0.5 to 3.0, the test data provides a good check for the design theory. In addition, since the girders were so large, the welding procedures adopted would be typical of those normally employed, thus the comparisons of the proposed design procedure with this experimental test data provides a most valuable check. It will be noted from Table 7 that very good correlation has been obtained between the shear failure load V_{RS} and the experimental loads. Since the I/b^3t ratio for the girders varies over a wide range, the influence of the flange flexibility parameter is well illustrated. It will be seen that the experimental ultimate load of girder G6 increase from 116 kips to 180 kips as the aspect ratio is decreased from 1.5 to 0.5, thus confirming the importance of the flange flexibility parameter.

Figures 3.7 and 3.8 or reference 9 (see also Figure 11 of Reference (7)), are particularly interesting since they show a section of girder G7 after tests T1 and T2 respectively. The mode of failure in both

cases being similar, as would be expected since the panels were nominally of identical size and subjected to identical loading. A distinct plastic hinge is visible in the compression flange of each of the panels. By making an enlargement of the picture, the approximate position of these hinges has been determined yielding c/b values of 0.3, this value being quite close to the value of c/b of 0.33 as obtained from the design procedure. In addition, Figure 3.21 of reference (9) shows the presence of the yield lines which developed in the compression flange of girder G7-T1 and from this figure a more accurate value of c/b equal to 0.33 has been obtained. The degree of agreement between this test data and the theoretical value being excellent. It is also of interest to note that whereas the plastic hinge in the compression flange is well developed, the hinges in the tension flanges are not so well defined, this again being in agreement with the findings of the authors.

In this present section, it has been fully established that the proposed design procedure for shear panels is capable of accurately predicting the failure load of such panels.

CONCLUSION

The paper presents an ultimate method of design for the collapse behaviour of plate girders loaded in shear which is substantiated by checking against experimental data.

ACKNOWLEDGEMENT

This research project has been sponsored in part by the Construction Industry Research and Information Association, in part by the British Constructional Steelwork Association and by the University College, Cardiff.

SYMBOLS

t	thickness of web plate
t_f	thickness of flange plate
d	clear depth of webplate between flanges
b	clear width of webplate between stiffeners
$\alpha = \frac{b}{d}$	aspect ratio of panel
I	flexural rigidity of flange members about an axis passing through their centroid and perpendicular to the web plate
V_{exp}	experimental ultimate shear load
V_{ult}	theoretical ultimate shear load
V_B	ultimate shear load provided by Basler collapse mechanism
V_F	ultimate shear load provided by Fujii
V_O	ultimate shear load provided by collapse mechanism proposed by Ostapenko and Chern
V_{RS}	ultimate shear load calculated by collapse mechanism presented by Authors
W	applied load
W_B	collapse load according to Basler mechanism

W_{cr} applied load resulting in buckling of webplate

W_{exp} experimental ultimate load

W_{RS} collapse load according to the Rockey, Skaloud collapse mechanism

τ applied shear stress

τ_{cr} critical shear stress $= K \frac{\pi^2}{12(1-\mu^2)} \left(\frac{t}{d}\right)^2$

where K is a non dimensional parameter

τ_{yw} shear yield stress of web material

τ_{ult} ultimate shear stress

α_{yw} tensile yield stress of web material

α_{yf} tensile yield stress of flange material

E Young's modulus of elasticity

υ Poisson's ratio

θ inclination of diagonal of panel with respect to flanges

BIBLIOGRAPHY

1. Leggett, D.M.A., & Hopkins, H.G., "The Effect of Flange Stiffness on the Stresses in a Plate Web Spar under Shear". H.M. Stationery Office, R & M No. 2434.
2. Bergman, S.G.A., "Behaviour of Buckled Rectangular Plates under the Action of Shearing Forces". Book. Stockholm, 1948.
3. Rockey, K.C., "The Influence of Flange Stiffness upon the Post Buckled Behaviour of Webplates subjected to Shear". Engineering. 20th Dec. 1957, 184, 788 - 792.
4. Djubek, J. "Stalbau Rundschau" Helt. 21-1962. Sonderheft, Osterreichische Stahlbautagung 1962. Innsbruck.
5. Rockey, K.C., & Martin, R.D., "Flange Stiffness and the Post Buckled Behaviour of Shear Webs". Civil Engineering Departmental Report, University College, Cardiff. 1967.
6. Basler, K., "Strength of Plate Girders". Ph.D. Thesis. Lehigh University, 1959.
7. Basler, K., "Strength of Plate Girders in Shear". A.S.C.E. Proc. No. 2967. ST. 7, p. 151, Octo. 1969. Part I.
8. Thurlimann, B., "Static Strength of Plate Girders". Extract Des Memoires de la Societe Royale des Sciences de Liege". Volume VIII. 1963, p. 137 - 175.
9. Basler, K., Yen, B.T., Mueller, J.A., & Thurlimann, B., "Web Buckling Tests on Welded Plate Girders". Welding Research Council Bulletin. No. 64. September 1960.
10. A.I.S.C. Specification. Adopted November 30th, 1961.
11. Rockey, K.C., "Factors Influencing Ultimate Behaviour of Plate Girders". Conference on Steel Bridges. June 24th-30th, 1968. British Constructional Steelwork Association, Institution of Civil Engineers, London.
12. Rockey, K.C., & Skaloud, M., "Influence of Flange Stiffness upon the Load Carrying Capacity of Webs in Shear". Final Report. 8th Congress New York, September, 1968. 11 pages.
13. Fujii, Tokyo. "On an Improved Theory for Dr. Basler's Theory". 8th Congress I.A.B.S.E. New York, 9-14th September, 1968. 9 pages.
14. Chern, C., & Ostapenko, A., "Ultimate Strength of Plate Girders

under Shear". Fritz Engineering Laboratory Report August, 1969. Report No. 328.7.

15. Rockey, K.C., "Ultimate Load Tests on Welded Shear Girders". Unpublished Report, 1958.
16. Rockey, K.C., & Skaloud, M., "The Ultimate Load Behaviour of Plate Girders Loaded in Shear". University College, Cardiff. Department of Civil Engineering Report - to be published.
17. Hu, P.C., Lundquist, E.R., & Batdorf, F.B., "The Effect of Small Deviations from Flatness on Effective Width and Buckling of Plates in Compression". N.A.C.A., T.N., p. 124. 1946.
18. Sakai, F., Doi, K., Nishino, F., & Okumwa, T., "Failure Tests of Plate Girders using Large Sized Models". Structural Engineering Laboratory Report. Department of Civil Engineering, University of Tokyo (1966). In Japanese.
19. Nishino, F., & Okumwa, T., "Experimental Investigation of Strength of Plate Girders in Shear". p. 451-462. 8th Congress I.A.B.S.E., New York, 1968.
20. Longbottom, E., & Heyman, J., "Experimental Verification of the Strengths of Plate Girders Designed in Accordance with the Revised British Standard 153 : Tests on Full Size and on Model Plate Girders". Inst. Civil Engineers, 1956.
21. Cook, I.T., & Rockey, K.C., "Shear Buckling of Rectangular Plates with Mixed Boundary Conditions". The Aeronautical Quarterly, Vol. XIV, March, 1963.
22. Bleich, F., "Buckling Strength of Metal Structures". McGraw Hill, 1952.
23. Rockey, K.C., "Ultimate Load Tests on Aluminium Plate Girders". Unpublished Research Data.

Leere Seite
Blank page
Page vide